Fachtagung "Experimentelle Strömungsmechanik"
5. – 7. September 2017, Karlsruhe

Strömungsvisualisierung der CO_2-Hydrat Bildung und Dissoziation

Flow visualization during CO_2-Hydrate formation-dissociation

J.R. Agudo[1], S. Kwon[1], R. Saur[1], S. Loekman[2], G. Luzi[1], C. Rauh[3], A. Wierschem[4], A. Delgado[1,4]

[1]Institute of Fluid Mechanics, FAU Busan Campus, University of Erlangen-Nuremberg,
46-742 Busan, Republic of Korea
[2]Institute of Chemical Reaction Engineering, FAU Busan Campus, University of Erlangen-Nuremberg,
46-742 Busan, Republic of Korea
[3]Department of Food Biotechnology and Food Process Engineering
Technische Universität Berlin
D-14195 Berlin, Germany
[4]Institute of Fluid Mechanics, University of Erlangen-Nuremberg,
D-91058 Erlangen, Germany

Methanhydrat, Umwelttechnik, Energietechnik.
Methane Hydrate, Green technology, Energy technology.

Abstract

During the last decade, Gas Hydrates (GHs) have attracted the interest of the scientific community. Carbon dioxide hydrate (CO_2H), for instance, may be of vital importance for capture and sequestration methods in order to reduce global climate change. The transport phenomena involved in the GH formation and dissociation process are not yet fully understood. Therefore, an exhaustive study is required to ensure a safe and ecological manipulation of GH.
In this study, we focus on GH dissociation process during depressurization. GH samples with different levels of gas saturation are illuminated with an impulse Nd: Yag laser and recorded with a CCD camera during dissociation at different water temperatures. We observe that the gas relief is characterized by a continuous dissociation column of microbubbles together with a sporadic relief of macro-bubbles with diameters ranging between 1 and 10 mm. The size of macro-bubbles depend on the initial gas saturation level of the samples. The total dissociation time is strongly affected by the water temperature. Beyond the effect of hydrate dissociation on the surrounding water, the dissolution of CO_2 in water is investigated using PIV. As CO_2 dissolved in the water phase, convective currents, caused by the density differences were observed. This process has shown a significant effect on the subsequent Hydrate formation from CO_2-saturated water.
Both the effect of dissociation on the surrounding fluid and the CO_2 dissolution process as a precursor to hydrate formation have to be taken into account when investigating the possible application of GH for CO_2 storage and CH_4 extraction.

Karlsruhe, Germany, ISBN 978-3-9816764-3-3

Introduction

Gas Hydrates (GHs) are crystalline solids consisting of gas molecules, also called guest or former molecules, enclosed in water cavities composed of hydrogen-bonded water molecules, also referred as host molecules [Sloan and Koh 2008]. Methane, ethane, propane or CO_2 are typical sorts of gas hydrate former. There is no bonding between frozen water and former gas molecules which are free to rotate inside the frozen water cage. The stabilization resulting from gas molecule is supposed to be due to van der Waals forces (attraction forces between molecules) and hydrogen bonds [Kahn 2011]. Given the enormous amounts of methane enclosed in form of hydrate that is encountered in deep ocean floors [Matsumoto et al. 2011], Methane Hydrates (MHs) are considered as one of the most important future source of hydrocarbon fuel [Max 2006].
Unlike MH, the existence of CO_2 Hydrates (CO_2Hs) as permanent disposal in Earth seems to be unrealistic as experimentally observed by [Brewer et al. 1999]. However, CO_2H is assumed to be abundant in the solar system playing a potential role in shaping the Martian landscape [Genov et al. 2005], or as a source of potable water for future human habitation [Pellenbarg et al. 2003]. Coming back to earthling applications, CO_2H formation-dissociation processes have recently attracted the interest of the scientific community for bioenergy applications. They are, for instance, of vital importance for CO_2 capture and sequestration methods, known as CCS. CCS are considered as one of the potential ways to reduce global climate change by preventing CO_2 gas emissions to the atmosphere. The first step of this process consists of separating CO_2 gas from exhaust emissions, coming for instance from fossil fuel power plants [Yang et al. 2012, Castellani et al. 2013]. Here, hydrated-base CO_2 separation points to a very promising alternative to current methods, e.g. absorption, adsorption, membrane separation or cryogenic fractionation [Kikkinides et al. 1993, Scondo and Sinquin 2011, Castellani et al. 2013, Babu et al. 2015] The last step of CCS process is the CO_2 storage into a safe and long-term system. Here, sequestering a large amount of CO_2 into deep ocean set-up have been recently contemplated in literature [Circone et al. 2003]. The replacement of CO_2 in marine MH deposits would permit CO_2 storage and release of methane as energetic input at the same time [Sivaraman et al. 2003, Castellani et al. 2013]. Other novel industrial applications include CO_2H-based water desalinization [Park et al. 2011, Babu et al. 2014, Kang et al. 2014] or CO_2H-based liquid concentration process for the food industry [Li et al. 2014, 2015]. To find a reliable, reproducible and efficient experimental method for GH production-dissociation process, is crucial for studying its viability in the aforementioned applications.
Despite the extensive literature, the transport phenomena involved during CO_2H formation are not yet fully understood. CO_2 transfer from gas or liquid phase to the bulk of water, for instance, is expected to happen not only by molecular diffusion but also driven by natural convective currents induced by CO_2 dissolution in water [Farajzadeh et al. 2007, 2009, Khosrokhavar et al. 2014]. These currents, that might play a key role in the CO_2 transport prior to hydrate formation, have not considered yet in classical mass transport models for CO_2H formation. Using particle tracer methods, we experimentally characterize the flow velocity of the bulk of water during CO_2H formation. For that purpose, CO_2H is grown inside an optical cell with a volume of 12 mL at various pressures and temperatures. Due to CO_2 dissolution, convection currents are noticed prior to hydrate formation. Our experimental results point to a significant correlation between this process and the subsequent hydrate formation.

Experimental set-up

CO_2H is formed in a cylindrical optical cell with a total volume of 12 mL designed for pressures up to 350 bars. The pressure cell contains four sapphire glasses for optical access and a cooling jacket to keep the temperature constant at 273.5 ± 0.5 K with the help of a circulating bath. The temperature is controlled with a K-type thermocouple coupled to the center of the cylindrical cell. The pressure is continually recorded outside the reactor by a pressure transducer within a relative uncertainty lower than 1%. Figure 1 illustrates the optical cell used for the experiments.

Karlsruhe, Germany, ISBN 978-3-9816764-3-3

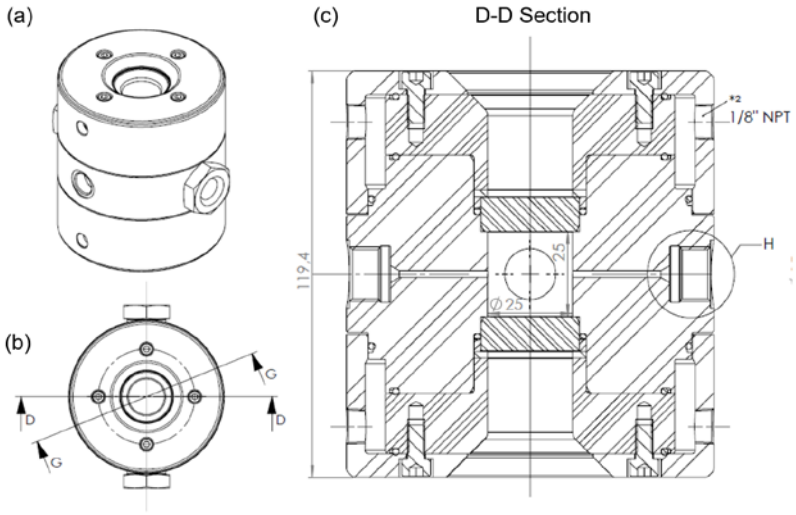

Fig. 1: Optical cell with a volume of 12 cm^3 and a total of four sapphire glasses used for the experiments (a). Top view (b) and vertical sectional view (c). The measurements are shown in mm.

To form CO_2H, 7 mL of deionized water (18.2 MΩ X cm of resistivity) is added first to the optical cell. After flushing the system, high purity CO_2 (99.95%) is injected into the vessel to achieve the proper pressure to form hydrate. Two different pressures were selected to form hydrate, 36 and 56 bars. The former is the equilibrium pressure between gaseous and liquid CO_2 at the operating temperature. Under this pressure, there are three phases in the reactor prior to hydrate formation: liquid water, liquid CO_2, and gaseous CO_2 from the bottom to the top in the reactor. The latter pressure corresponds to the maximum provided by the CO_2 bottle at the same temperature. In this case, only liquid water and liquid CO_2 are encountered in the reactor before hydrate formation.

To characterize the flow in the bulk of water, the water is seeded with Polyamide Seeding Particles (PSP) of 5 microns diameter. Given the long-term duration of the experiments, up to 48 hours for hydrate formation, a continuous cold LED source of 55 W with a light guide of 15 mm in diameter is selected for the volume illumination of the cell. The use of this low power light source showed a marginal impact on the bulk temperature and allows us to continue the particle image velocimetry (PIV) measurements in the bulk of water once the hydrate growths in the interface. Two different imaging systems are simultaneously used for conducting the measurements. A 1280 x 1024 CMOS camera coupled to an 180 mm, f/3.5 Macro lens is used for recording from the front at a working distance of 730 mm from the center of the cylindrical cell. The field of view, in this case, is a circular window of 15 mm in diameter which corresponds to the dimensions of the sapphire glass integrated into the side of the reactor. A 1920 x 1080 CMOS camera equipped with a modular zoom lens system that incorporates a tilted mirror is used for recording from the back. The working distance is 53 mm. The magnification of the lens system ranges between M = 1.1 and M = 7.8, and the numerical aperture between NA = 0.036 and NA = 0.12, respectively. The field of view ranges between 4.2 x 5.6 and 0.61 x 0.81 mm, while the depth of field ranges between 0.42 and 0.038 mm, respectively. Figure 2 illustrates the experimental set-up. While the front camera is used to measure the flow velocity in the entire bulk of water (see Figure 3), the back camera permits us to focus on the interface, where hydrate formation is likely to happen (see Figure 4). For the front and the back system, the images are recorded at a video rate of 2 and 5 Hz, respectively. The particle image fields are analyzed by classical cross-correlation implemented by fast Fourier transform using Insight4G®. The size of the interrogation area is 32 x 32 pixels in both systems. This corresponds to a spatial resolution of approximately 0.4 mm in the front system. Defining a peak to noise peak ratio of 1.47, the analyzed particle-image fields reveal typical ratios of good vectors above 80%. The PIV analysis, however, produces a few obvious false positive velocities vectors which are several orders of magnitudes larger than the average. Additionally, all points outside of the processing mask are

zero. Thus, to remove the false positive values, every point with a velocity above the 95%-tile of non-zero velocities were cut. When calculating the average velocity at a specific point in time, only non-zero velocities were considered. In order to improve readability, the velocities were averaged over 60 seconds.

The accuracy of the PIV system installed in the back was checked with the known solution of a Couette flow velocity profile induced by an MCR302 rotational rheometer with a parallel-disk configuration. A circular container with transparent Plexiglas sidewalls and a chamfer in the front was concentrically coupled to the rheometer. For more details in this experimental set-up, we refer to [Agudo and Wierschem 2012, Agudo et al. 2014]. The distance from the rotating plate to the surface is fixed at 2 mm and the angular frequency of the rotating plate was set to obtain velocities of the order than those observed during GH formation experiments. The PIV measurements revealed a deviation lower than 5% with respect to the expected flow velocity confined between the plates. A comparison in velocity between the front and the back PIV system showed typical deviations lower than 10%.

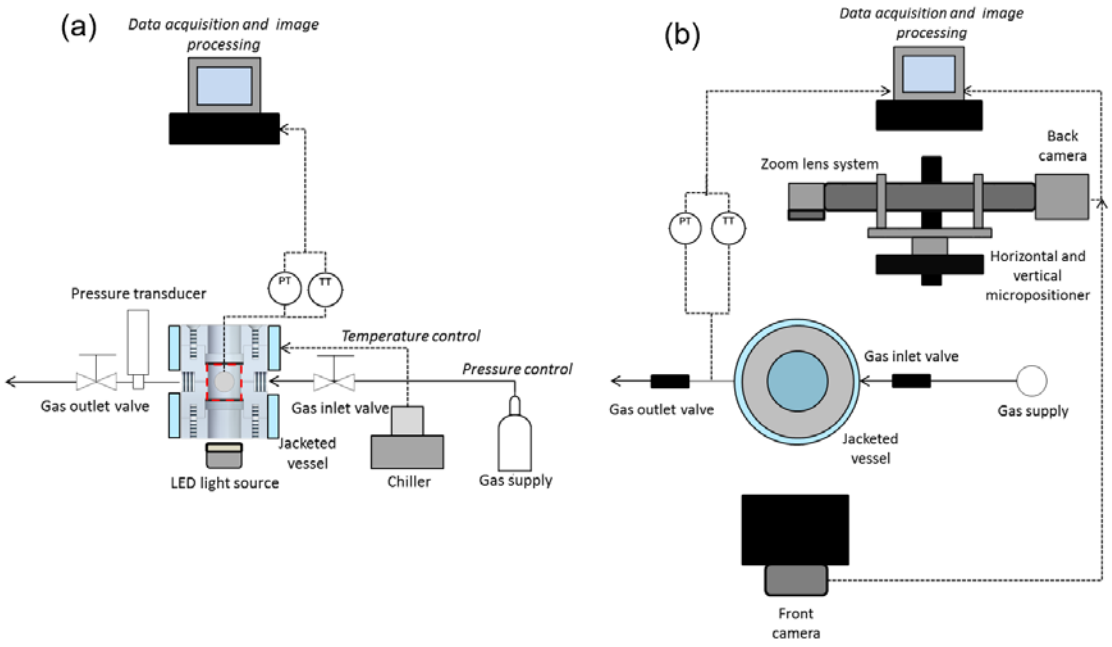

Fig. 2: Sketch of the experimental set-up for PIV measurements during CO_2 hydrate formation. Front view (a) and top view (b).

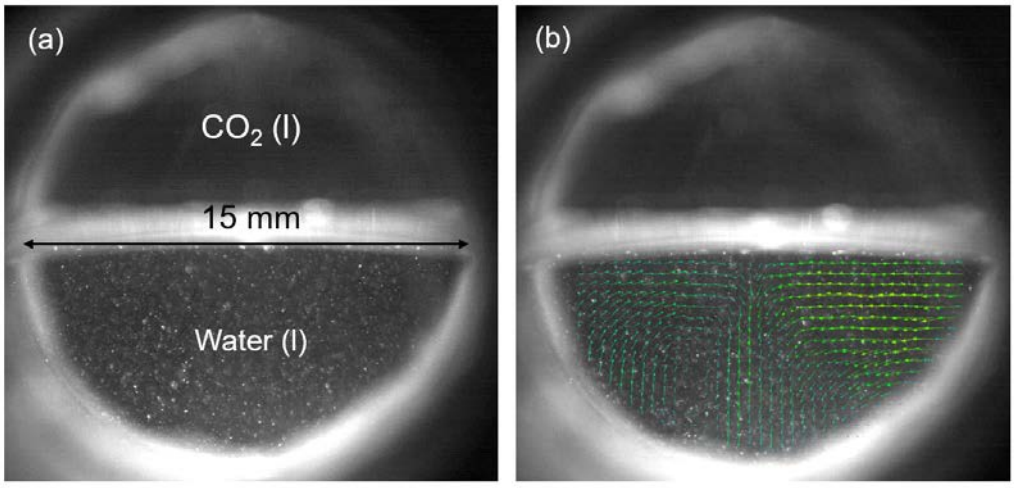

Fig. 3: Digital image of the seeded flow inside the optical cell recorded from the front imaging system at 56 bar and 273.5 K (a). Velocity vector maps obtained by the aforementioned system prior to hydrate formation (b).

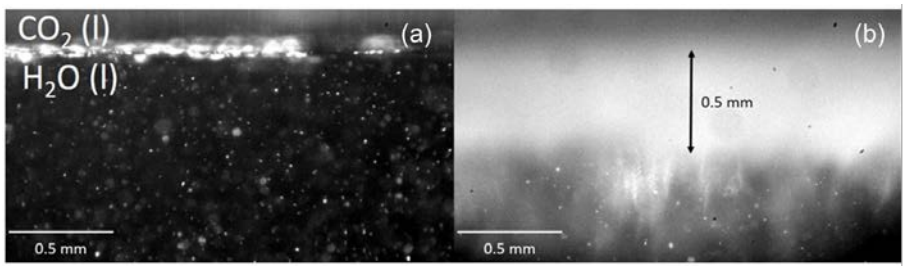

Fig. 4: Digital image of the seeded flow inside the optical cell recorded from the back imaging system at 56 bars and 273.5 K prior to hydrate formation (a). Frame representing the onset of hydrate formation in the experiment.

Results and discussion

In a system as shown in Figure 3, CO_2 is first expected to dissolve into the water phase by molecular diffusion through the interface [Farajzadeh et al. 2009]. Since the dissolution of CO_2 increases the density of water [Gmelin 1973], a gradient of density is expected to induce the instability of the boundary layer saturated with CO_2 [Farajzadeh et al. 2007, 2009]. This instability yields in recirculation flows as shown in Figure 3(b). The criteria to predict the existence of the natural convection is usually characterized by the Rayleigh number, which depends on the fluid properties and geometry dimensions. The Rayleigh number can be defined as [Farajzadeh et al. 2009, Khosrokhavar et al. 2014]:

$$Ra = \frac{\Delta\rho g R^3}{\rho_i \nu D} \tag{1}$$

where $\Delta\rho$ is the gradient of density of the fluid, g is the gravity acceleration, R is the radius of the cylindrical cell, ρ_i is the initial density of water, ν is the kinematic viscosity of water and D is the diffusion coefficient of water. Natural convection typically occurs when Ra>2100 [Khosrokhavar et al. 2014]. The other independent dimensionless number that governs the flow is the Re numbers defined as:

$$\mathrm{Re} = \frac{uR}{\nu} \tag{2}$$

where u is the maximum in-plane velocity registered by the PIV system. At similar pressure conditions than in our experiments, gradients of density driven by CO_2 dissolution up to 8 kg/m^3 has been reported in literature [Khosrokhavar et al. 2014]. Accordingly, Rayleigh numbers of the order of 10^7 are expected in our system, and buoyancy-driven convection is likely to happen prior to hydrate formation in the reactor. On the other hand, with maximum measured velocities of about 0.2 mm/s, the Reynolds number remains below 2 in our experiments indicating the existence of laminar flows.

Two preliminary experiments are conducted to clarify that buoyancy-driven convection due to CO_2 dissolution is the main cause of induced-flow currents before hydrate is formed in the optical cell. In a first experiment, CO_2 is injected into the reactor at the operating temperature to an initial pressure of 32 bars. Pressure, temperature and averaged velocities in the bulk of water are recorded simultaneously. Figure 5 depicts the results. The data are plotted up to 6 hours. No hydrate formation was noticed during that time. Pressure and average velocity experience a gradually decrease with time until a plateau at about 5 hours is reached. The temperature increases by approximately 1 K as a consequence of the increment of pressure. Unlike the long-term decrease of pressure with time, the measured temperature reaches a constant plateau after approximately 1 min, and keep constant during the rest of the experiment (see inset of Figure 5(a)). Since the temperature remains constant, the pressure drop in the system is mainly due to CO_2 dissolution in water [Silva et al. 2013].

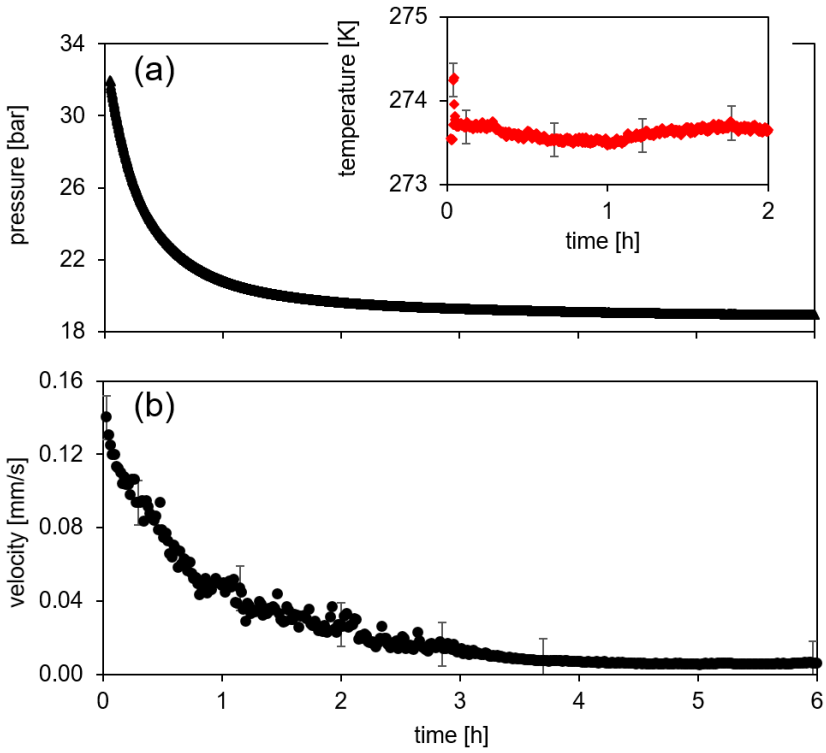

Fig. 5: Pressure (a) and averaged velocity in the bulk of water (b) as a function of time. The inset depicts the temperature as a function of time. Experiment performed with 7 mL of water and CO_2 at 36 bars and 273.5 K.

Comparison between pressure and velocity trends show a remarkable similarity between each other. This indicates that CO_2 dissolving in the bulk of water but not fluctuations in temperature is the main source of the density-driven natural convection. Note that a constant pressure in the system indicates that equilibrium conditions for CO_2 solubility in the bulk of water has been achieved at the corresponding pressure and temperature. No gradient of CO_2 concentration exists in the bulk of water, and convection currents disappear as shown in Figure 5(b).

To check that flow velocities are not driven by mechanical agitation after an increase of pressure, a second experiment is conducted by injecting water non-soluble gas helium (He) up to 56 bars at operating temperature. Open symbols in Figure 6 represent the averaged flow velocity as a function of time. Solid symbols depict the averaged velocity for an experiment performed with CO_2 at same conditions. The experiment performed with CO_2 reveals again a gradual decrease of velocity until a plateau is achieved after about 5 hours. The averaged velocity in the experiment conducted with He drops to the same value but immediately after the pressure is increased in the optical cell. The pressurization and the corresponding velocity measurements for the experiment performed with He can be seen in Figure 6(b) and (c), respectively. The red line indicates the instant in which the pressure is increased in the system. From Figure 6(c) it is clear that although increasing the pressure induces some initial movement, the effect dies down after a few seconds. This corroborates that without the dissolution-driven Rayleigh convection the measured velocities are significantly lower. Note that convection induced by a temperature gradient should still be visible when using a non-soluble gas.

The trend of velocity in the experiment performed with CO_2 at 56 bars is very similar to that observed at 32 bars (see Figure 5(b)). This can be explained by the fact that solubility isopleths of CO_2 hardly increases with pressure at operating temperature (see for instance P-T diagram for CO_2 solubility by [Diamond and Akinfiev 2003]). This indicates that similar gradient of densities are expected at saturated and supersaturated conditions.

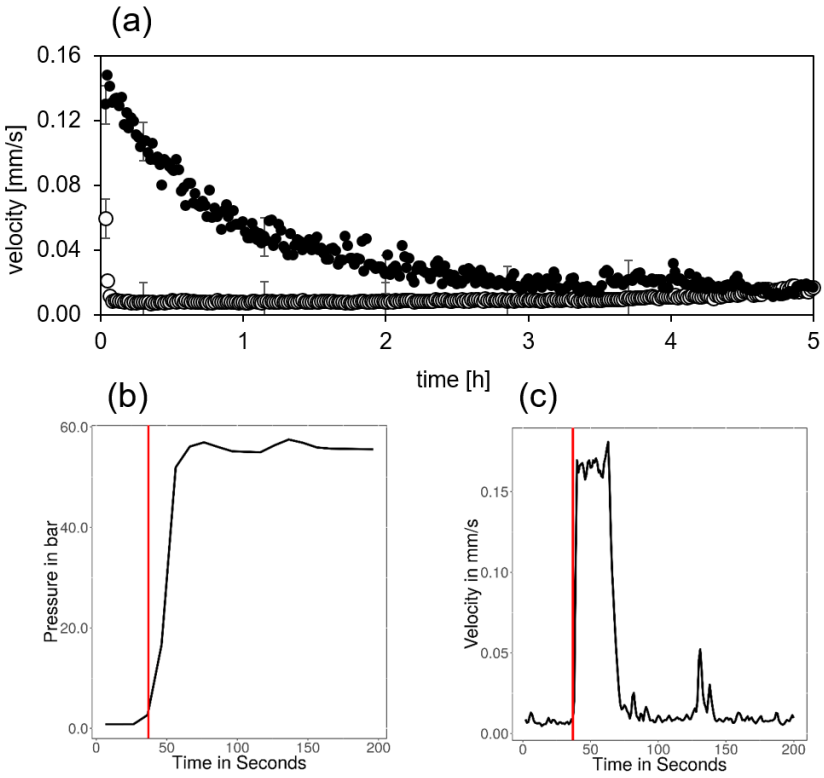

Fig. 6: Averaged velocity in the bulk of water as a function of time (a). Solid and open symbols represent experiments performed with CO_2 and He, respectively. Experiments performed with 7 mL of water at 56 bar and 273.5 K. Pressure (a) and averaged velocity (b) right after increase of pressure for the experiment conducted with He.

Conclusions

We characterize the flow velocity field of the bulk of water during CO_2H formation in an optical cell with a volume of 12 mL filled with 7 mL of deionized water. For that purpose, two different imaging systems are simultaneously used for recording the particle-image fields from the front and the back, respectively. Classical PIV analysis is performed to obtain the map of velocity vectors. The system on the back, with a higher spatial resolution, is used to focus on the interface where hydrate is expected to form. The system from the front is used to analyze the velocity on the entire bulk of water. Recirculation flows are noticed as a consequence of density-driven natural convection. We observe a gradual decrease of the averaged velocity with time as a consequence of this phenomenon. In a first experiment performed with gas CO_2 and liquid water, both pressure and averaged velocity drop shows a very similar trend while the temperature remains constant in the cell. A second experiment performed with helium, a non – soluble gas in water, reveals that unlike experiments performed with CO_2, the velocity drop is instantaneous in the system after an increase of pressure. In view of these results, we assume that the driven natural convection is mainly induced by CO_2 dissolution into the bulk of water, but not by fluctuations in temperature nor mechanical agitation as a consequence of the increase of pressure in the system.

Literature

Agudo, J.R., Wierschem, A., 2012: “Influence of the substrate geometry on the onset of particle motion at low particle Reynolds numbers”, Phys. Fluids. 093302, 24.
Agudo, J.R., Dasilva, S., Wierschem, A. 2014: “How do neighbors affect incipient particle motion in shear flows?”, Phys. Fluids. 053303, 26.
Babu, P., Kumar, R., Linga, P., 2014: “Unusual behavior of propane as a co-guest during hydrate formation in silica sand: Potential application to seawater desalination and carbon dioxide capture”, Desalination, 274, pp. 91-96.

Babu, P., Linga, P., Kumar, R., Englezos P., 2015: “A review of the hydrate based gas separation (HBGS) process for carbon dioxide pre-combustion capture”, Energy, 85, pp. 261-279.
Brewer, P.G., Friederich, G., Peltzer, E. T., Orr Jr., F.M., 1999: “Direct Experiments on the Ocean Disposal of Fossil Fuel CO2”, Science, 284, pp. 943-945.
Castellani, B., Filipponi, M., Nicolini, A., Cotana, F., Rossi, F., 2003: “Carbon Dioxide Capture Using Gas Hydrate Technology”, Journal of Energy and Power Engineering, 7, pp. 883-890.
Diamond, W. L., Akinfiev, N. N., 2003: “Solubility of CO_2 in water from -1.5 to 100°C and from 0.1 to 100 MPa: evaluation of literature data and themodynamic modelling”, Fluid Phase Equilibria, 208, pp. 265-290.
Farajzadeh, R., Hamidreza, S., Zitha, P. L. J., Bruining, H., 2007: “Numerical simulation of density-driven natural convection in porous media with application for CO_2 injection projects”, Int. J. Heat Mass Transfer,50, pp. 5054-5064.
Farajzadeh, S., Zitha, P. L. J., Bruining, H., 2009: “Enhanced Mass Transfer of CO2 into Water: Experiment and Modeling”, Ind. Eng. Chem. Res., 48, pp. 6423-6431.
Gmelin, L., 1973: “Gmelin Handbuch der anorganischen Chemie, 8; Auflage. Kohlenstoff, Teil C3, Verbindungen.
Genov, G., Falenty, A., Kuhs, E. T., Orr Jr., F.M., 2005: “The possible role of CO2 hydrates for terra-forming processes on Mars”, in Proceedings of European Geosciences Union 2005 (EGU 2005), 7, 05532.
Kang, K. C., Linga, P., Park, K., Choi, S.J., Lee, J.D., 2014: “Seawater desalination by gas hydrate process and removal characteristics of dissolved ions (Na+, K+, Mg2+, Ca2+, Cl- ,SO42-)”, Desalination, 353, pp. 84-90.
Khan, M.R., 2011: “Advances in clean hydrocarbon fuel processing: Science and technology”, Cambridge: Woodhead Publishing Limited.
Khosrokhavar, R., Elsinga, G., Farajzadeh, R., Bruining H., 2014: “Visualization and investigation of natural convection flow of CO_2 in aqueous and oleic systems”, J. Pet. Sci. Eng., 122, pp. 230-329.
Kikkinides, E.S., Yang, R.T., Cho S.H., 1993: “Concentration and recovery of CO2 from flue-gas by pressure swing adsorption”, Ind. Eng. Chem., 32, pp. 2714-2720.
Li, S., Shen, Y., Dongbing, L., Fan, L., Zhang, Z, Li, W., 2014: “A Novel Orange Juice Concentration Method Based on C2H4 Clathrate Hydrate Formation”, Advance Journal of Food Science and Technology, Bd. 6, 6, pp. 780-783.
Li, S., Shen, Y., Dongbing, L., Fan, L., Tan, Z., 2015: “Concentration orange juice through CO2 clathrate hydrate technology”, Chemical Engineering Research and Design, 93, pp. 773-778.
Matsumoto, R., Ryu, B.J., Lee, S.R., Lin, S., Wu, S., Sain, K., Pecher, I., Riedel, M., 2011: “Occurrence and exploration of gas hydrate in the marginal seas and continental margin of the Asia and Oceania region”, Mar. Petrol. Geol., 28, pp. 1751-1767.
Max, N. D., Johnson, A. H., Dillon, W. P., 2006: “Economic Geology of Natural Gas Hydrate”, Dordrecht: Springer.
Park, K., Hong, S. Y., Lee, J.W., Kang, K.C., Lee, Y.C., Ha M.G., Lee, J.D., 2011: “A new apparatus for seawater desalination by gas hydrate process and removal characteristics of dissolved minerals (Na+, Mg2+, Ca2+, K+, B3+)”, Desalination, 274, pp. 91-96.
Pellenbarg, R.E., Max, M.D., Clifford, S. M., 2003: “Methane and carbon dioxide hydrates on Mars: Potential origins, distribution, detection, and implications for future in situ resource utilization”, Journal of Geophysical Research, 108, E4, pp. 2156-2202.
Scondo, A., Sinquin, A., 2011: “Effect of additives on CO2 capture from simulated flue gas by hydrates formation in emulsion”, in: 7th International Conference on Gas Hydrates, Edinburgh, Scotland, UK, 2011.
Sivaraman, R., 2003: “The potential Role of Hydrate Technology in Sequestering Carbon Dioxide”, Gas TIPS News Letter, Fall 2003, Gas Technology Inst.
Silva Lirio, C. F. da, Pessoa, F. L. P., Uller, A. M. C., 2013: “Storage capacity of carbon dioxide hydrates in the presence of sodium dodecyl sulfate (sds) and tetrahydrofuran (thf)”, Chem. Eng. Sci., 96,118123.
Sloan, E. D., Koh, A. C., 2008: “Clathrate Hydrates of Natural Gases”, CRC Press, New York.
Yang, M., Song, Y., Ruan, X., Liu, L., Zhao, J., Li, Q., 2012: “Characteristics of CO2 Hydrate Formation and Dissociation in Glass Beads and Silica Gel”, Energies, 5, pp. 925-937.